

will slow down the inversion at low temperatures. There the rotation will proceed by tunneling, which suggests that at low temperatures the inversion may show evidence of a substantial deuterium effect. Unfortunately no experimental data are available to test this suggestion.

The calculations allow an assessment of the contribution of tunneling transfer to the inversion. To this end, we have repeated the calculations including only over-the-barrier transitions. The results are represented by the broken line in Figure 3. They show that tunneling is not negligible for the inversion but becomes the dominant transfer mechanism for $T \leq 110$ K. As pointed out above, the overestimate of the transfer rate at 94 K is ascribed

to the neglect of methyl rotation and should not be interpreted as support for an over-the-barrier mechanism.

The argument presented here is general and should apply to many other inversion processes involving a methyl group. These processes are expected to be slow and deuterium sensitive at low temperatures where tunneling becomes dominant. In the absence of experimental data this conclusion must take the form of a prediction.

Acknowledgment. We thank Keith Ingold for his interest in this work and numerous helpful discussions.

Registry No. Methylcyclopropyl radical, 2154-76-9.

^{51}V NMR as a Probe of Vanadium(V) Coordination to Human Apotransferrin

Alison Butler* and Hellmut Eckert

Contribution from the Department of Chemistry, University of California, Santa Barbara, California 93106. Received January 13, 1988

Abstract: ^{51}V NMR is a highly sensitive tool to probe the nature of the metal binding sites of human transferrin (Tf). At a field strength of 11.7 T, the two vanadium(V) binding sites in $\text{V}_2\text{-Tf}$ are characterized by ^{51}V chemical shifts at -529.5 and -531.5 ppm versus VOCl_3 . These shifts are assigned to the C- and N-terminal sites, respectively, based on the ^{51}V NMR spectra of vanadate addition to $\text{Fe}_\text{N}\text{-Tf}$ and $\text{Fe}_\text{C}\text{-Tf}$. Tight binding of V(V) to the metal binding site is further ascertained by a linear increase of signal area with V(V) concentration up to an approximate 2:1 stoichiometry, stoichiometric displacement of protein-bound V(V) during titration with Fe(III), and the absence of the $-529.5/-531.5$ ppm resonance upon addition of V(V) to Fe_2Tf and Ga_2Tf . The chemical shift of the $\text{V}_\text{C}\text{-Tf}$ resonance is independent of pH (5.8–9.0) and temperature (275–310 K), whereas the $\text{V}_\text{N}\text{-Tf}$ resonance varies slightly (1–2 ppm) with pH and temperature. At relatively high V(V) concentrations and at high ratios of V(V)/Tf, conditions under which a large fraction of the V(V) is present as V oligomers, the ^{51}V resonance of Tf-bound V(V) is not observed, possibly owing to interference by the oligomeric species. Under conditions of tight V(V) binding, the sharpness of the protein-bound resonances is a consequence of the motional characteristics of transferrin, which place the Tf-bound vanadium(V) outside the extreme narrowing limit but within the motional narrowing limit. Several theoretically predicted consequences for an $I = 7/2$ nucleus are observed experimentally, some for the first time in an aqueous protein system. (1) The observed signal intensity of transferrin-bound vanadium(V) compared to that of an equimolar aqueous vanadate sample is substantially reduced, since only one out of four spin-spin relaxation components (i.e., $+1/2 \rightarrow -1/2$ transition) is observed. (2) At 7.05 T the line width is substantially greater than at 11.7 T, and a 5-ppm upfield shift is observed which is attributed to a dynamic frequency shift. (3) The line width of Tf-bound V(V) is not affected by solvent viscosity up to 50% v/v glycerol/buffer. (4) Measurements of signal intensity as a function of pulse length reveal increased ^{51}V precession frequencies in the radio-frequency field, as frequently observed for half-integer quadrupolar nuclei in the solid state. The excitation spectrum is found to be identical for V_C and V_N sites and independent of the V/Tf ratio. At small pulse angles, the fraction of the signal observed is constant and amounts to ca. 20% of that of an equimolar solution of free vanadate, in close agreement with the theoretical prediction. The present study confirms that ^{51}V NMR is a powerful tool to probe V(V) binding to apotransferrin and should also become widely applicable to characterize V(V) binding to other macromolecules.

Transferrins are glycoproteins whose primary function is to bind and transport iron. Transferrins also coordinate a wide variety of other metal ions (e.g., Cu(II), VO^{2+} , Cr(III), Ga(III), Tl(III), etc.),¹ including vanadium(V).²⁻⁴ Human transferrin (Tf) is a single polypeptide chain with two homologous regions each of which binds one metal atom.¹ Elucidation of the similarities and differences between the two metal binding sites continues to be an area of active interest, the results of which should increase our understanding of the functional differences of the two binding sites. The X-ray crystal structure of human lactoferrin shows that the iron binding sites are separated by 42 Å and that the metal binding

ligands at *both* binding sites are two tyrosine residues, one histidine residue, one aspartate residue, a H_2O (or OH^-) molecule, and an anion (CO_3^{2-} or HCO_3^-).⁵ The fact that human transferrin and lactoferrin share a high degree of sequence homology ($\sim 30\%$),^{1c} that all the metal binding amino acids in lactoferrin are conserved in human transferrin, and that much spectroscopic evidence indicates that the binding sites of lactoferrin and human transferrin are similar, suggests that the metal binding ligands are the same between transferrin and lactoferrin *and* between the two metal binding sites in human transferrin.

A wide variety of experimental results, however, suggest the two metal binding sites in human transferrin are not *equivalent*, even though the ligands of both sites may be identical. Structural differences have been inferred from the ESR spectra of the Fe(III)-,⁶ VO^{2+} -,⁷ Cu(II)-, and Cr(III)-bound⁸ transferrin derivatives

(1) (a) Chasteen, N. D. *Adv. Inorg. Biochem.* **1983**, 58 201. (b) Aisen, P.; Listowsky, I. *Annu. Rev. Biochem.* **1980**, 49, 357. (c) Brock, J. H. in *Metalloproteins*; Harrison, P. M., Ed.; Verlag Chemie: Weinheim, West Germany, 1985; Part 2, p 183 and references therein.

(2) Harris, W. R.; Carrano, C. J. *J. Inorg. Biochem.* **1984**, 22, 201.

(3) Chasteen, N. D.; Grady, J. K.; Holloway, C. E. *Inorg. Chem.* **1986**, 25, 2754.

(4) Butler, A.; Danzitz, M. J.; Eckert, H. *J. Am. Chem. Soc.* **1987**, 109, 1864.

(5) Anderson, B. F.; Baker, H. M.; Dodson, E. J.; Norris, G. E.; Rumball, S. V.; Waters, J. M.; Baker, E. D. *Proc. Natl. Acad. Sci. U.S.A.* **1987**, 84, 1769-1773.

(6) Aisen, P.; Liebman, A.; Zweier, J. J. *Biol. Chem.* **1978**, 253, 1930.

and the ^{205}Tl NMR spectrum of Tl_2 transferrin.⁹ Iron binding and release at the two sites has been found to be affected by pH, with the C-terminal site binding Fe(III) preferentially at pH 5.8.^{10-12,27} We have shown that the two vanadium-binding sites in V(V)-bound human transferrin can be distinguished using ^{51}V NMR.⁴

Until recently, the outstandingly favorable NMR properties of the ^{51}V NMR isotope had not been fully appreciated for the study of vanadium(V)-protein interactions.^{4,13} ^{51}V NMR is emerging as an excellent diagnostic tool for detailed investigations of vanadium(V) coordination environments, because the chemical shifts are very sensitive to changes in the nature of the coordination environment.¹⁴⁻¹⁸ In addition, the large magnetic moment of ^{51}V , its high natural abundance (99.76%), and its favorable relaxation properties (see below) should enable the use of ^{51}V NMR as a selective probe of vanadium bound to macromolecules. As has been demonstrated for other quadrupolar nuclei, the quadrupolar relaxation behavior is a source of information about the nature of the coordination ligands, exchange kinetics, and the motional properties of the macromolecule.¹⁹⁻²¹

Several applications of ^{51}V NMR to probe vanadium(V)-protein interactions can be found in the literature.^{4,13,22-25} In most of these cases,^{13,22-25} the resonance of the protein-bound vanadium was either extremely broad or not observed at all. In contrast, the ^{51}V NMR resonances of V(V) bound to transferrin are sharp and permit chemical shift discrimination of the two metal binding sites. As suggested in our previous communication, this unusual situation results from the motional properties of the protein-bound vanadate, which fall outside the extreme narrowing limit. This situation results in signal intensity loss as well as comparatively sharp resonance lines because only one component (i.e., $+1/2 \rightarrow -1/2$ transition) of a multiexponential spin-spin relaxation decay is observed, while the other three components are broadened beyond detectability. In the present study we have characterized this "non-extreme-narrowing condition" by a detailed account of experiments involving the effects of solvent viscosity, temperature, and external magnetic field strength on line widths and resonance shifts, as well as measurements of the effective precession frequencies of the quadrupolar ^{51}V nuclei in the applied radio-frequency field. Implications of the latter effect for quantitative ^{51}V NMR spectroscopic applications are examined. We have also expanded our investigation of the chemical conditions affecting vanadate binding to human apotransferrin, Fe_N -Tf and Fe_C -Tf, the results of which further substantiate our initial observations that the two protein-bound ^{51}V signals characterize distinct binding sites.

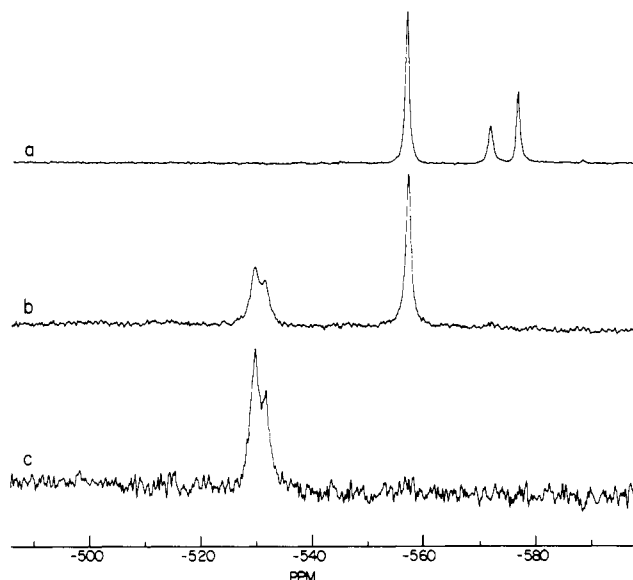


Figure 1. ^{51}V NMR spectra of vanadate-bound Tf and aqueous vanadate at pH 7.4, 0.1 M Hepes buffer, 131.48 MHz: (a) 0.826 mM aqueous vanadate, 26 342 scans; (b) 2.3:1 M/M mixture of V(V) and apo-Tf at 0.826 mM apo-Tf, 205 159 scans; (c) equimolar mixture of V(V) and apo-Tf at 0.34 mM, 200 010 scans.

Experimental Section

Sample Preparation and Characterization. Apotransferrin obtained from Calbiochem or Sigma was purified by extensive dialysis against 0.1 M aqueous NaClO_4 .²⁶ In some experiments the apotransferrin was incubated with 50 mM vanadate to oxidize spurious reducing agents and then dialyzed extensively against buffer to remove excess vanadate, yielding the V(V)₂-transferrin derivative.³ The C-terminal monoferric transferrin derivative, Fe_C -Tf, and the N-terminal monoferric derivative, Fe_N -Tf, were prepared according to published procedures.²⁶ Urea/polyacrylamide gel electrophoresis was used to confirm that Fe_C -Tf and Fe_N -Tf had been correctly synthesized.²⁷

Samples were studied in the pH range 5-9, using appropriate buffer solutions of 0.1 M Hepes (*N*-2-(hydroxyethyl)piperazine-*N'*-2-ethanesulfonic acid), Bicine (*N,N*-bis(2-hydroxyethyl)glycine), or Mes (2-(*N*-morpholino)ethanesulfonic acid). Stock solutions of vanadate were kept below 20 mM total vanadium at pH 7.5 to avoid the formation of decaavanadate.

V-51 NMR. The NMR experiments were done at room temperature using Bruker WM and AM-500, and General Electric GN 500- (frequency for ^{51}V , 131.5 MHz) and 300-MHz (frequency for ^{51}V , 79.0 MHz) spectrometers equipped with multinuclear broadband probes. Spectra were acquired unlocked, in nonspinning samples, under the following conditions: 90° pulse length 30-45 μs for an aqueous vanadate solution (depending on the spectrometer), pulse repetition rate 10-50 ms, spectral width 100 000 Hz. Additional experiments were performed at 79.0 MHz using a Chemagnetics high-power solid-state NMR probe (9- μs 90° pulse on an aqueous vanadate solution). Typically about 200 000 scans were necessary to obtain an acceptable signal-to-noise ratio on a 0.1 mM V-transferrin solution. The free induction decays were zero-filled to 16 K and multiplied by an exponential filter function equivalent to a line-broadening of 20 Hz prior to Fourier transformation. Chemical shifts are reported relative to neat VOCl_3 as an external reference.

Results and Interpretation

Coordination of Vanadate to Human Apotransferrin. Figure 1 shows the ^{51}V NMR spectrum of a solution of NH_4VO_3 dissolved in Hepes buffer in the presence and absence of apotransferrin. The spectrum of the aqueous vanadate solution (Figure 1a) shows the resonances which have been previously assigned to $\text{H}_2\text{VO}_4^-/\text{HVO}_4^{2-}$ (-555 to -560 ppm), $\text{H}_2\text{V}_2\text{O}_7^{2-}$ (-567 to -571 ppm), and a tetravanadate species (-576 ppm), respectively.^{16,17} Upon addition of 1 equiv of transferrin, the total signal intensity decreases to ca. 15-20%, and two new overlapping resonances at -529.5 and -531.5 ppm (relative to VOCl_3) are observed, with

(7) Cannon, J. C.; Chasteen, N. D. *Biochemistry* **1975**, *14*, 4573.

(8) Harris, D. C. *Biochemistry* **1977**, *16*, 560.

(9) Bertini, I.; Luchinat, C.; Messori, L. *J. Am. Chem. Soc.* **1983**, *105*, 1347.

(10) The amino acid sequence comprising residues 1-336 contains the "N-terminal binding site", and it is 42% homologous with residue sequence 337-679, which contains the "C-terminal binding site".¹ The "N- or C-terminal" terminology does not imply coordination to the terminal amino acid residues.¹

(11) Aisen, P.; Liebman, A.; Zweier, J. J. *Biol. Chem.* **1978**, *253*, 1930.

(12) (a) Evans, R. W.; Williams, J. *Biochem. J.* **1978**, *173*, 543. (b) Zapolski, E. J.; Princiotta, J. V. *Biochemistry* **1980**, *19*, 3599.

(13) Vilter, H.; Rehder, D. *Inorg. Chim. Acta* **1987**, *136*, L7.

(14) Gresser, M. J.; Tracey, A. S.; Parkinson, K. M. *Inorg. Chem.* **1987**, *26*, 629.

(15) Habayeb, M. A.; Hileman, O. E., Jr. *Can. J. Chem.* **1980**, *58*, 2255.

(16) Heath, E.; Howarth, O. W. *J. Chem. Soc., Dalton Trans.* **1981**, 1105.

(17) Rehder, D. *Bull. Magn. Reson.* **1982**, *4*, 33.

(18) Gresser, M. J.; Tracey, A. S. *J. Am. Chem. Soc.* **1986**, *108*, 6229.

(19) Forsen, S.; Lindman, B. *Methods Biochem. Anal.* **1981**, *27*, 289.

(20) Drakenberg, T.; Forsen, S.; Lilia, H. *J. Magn. Reson.* **1983**, *53*, 412.

(21) Drakenberg, T.; Andersson, T.; Forsen, S.; Wieloch, T. *Biochemistry* **1984**, *23*, 2387.

(22) Cserehely, P.; Martonosi, A.; Levy, G. C.; Ejchart, A. J. *Biochem. J.* **1985**, *230*, 807.

(23) Stankiewicz, P. J.; Gresser, M. J.; Tracey, A. S.; Hass, L. F. *Biochemistry* **1987**, *26*, 1264.

(24) Borah, B.; Chen, C.-W.; Egan, W.; Miller, M.; Wlodawer, A.; Cohen, J. S. *Biochemistry* **1985**, *24*, 2058.

(25) Sakurai, I.; Nishida, M.; Kida, K.; Koyama, M.; Takada, J. *Inorg. Chim. Acta* **1987**, *138*, 149.

(26) Folajtar, D. A.; Chasteen, N. D. *J. Am. Chem. Soc.* **1982**, *104*, 5775.

(27) Mackey, D. G.; Seal, U. S. *Biochim. Biophys. Acta* **1976**, *453*, 250.

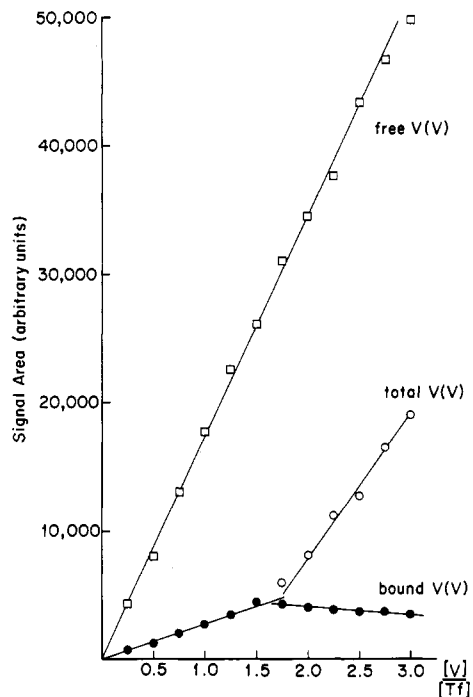


Figure 2. ^{51}V NMR titration (131.48 MHz) of 0.62 mM apo-Tf with vanadate, pH 7.4, 0.1 M Hepes (a) versus equivalent titration in the absence of apo-Tf (b).

a total line width of 420 Hz (Figure 1c). Upon addition of a second equivalent of vanadate (Figure 1b), the presence of some $\text{H}_2\text{VO}_4^-/\text{HVO}_4^{2-}$ (-556 ppm) is evident. Because of the intrinsically lower signal intensity of the protein-bound vanadate (see below), the amount of free vanadate in Figure 1b is actually very small compared to that of the protein-bound vanadate. To confirm that the signals at -529.5 and -531.5 ppm arise from protein-bound V(V), the signal areas of these resonances were measured as a function of incremental addition of vanadate to the apoprotein. This titration study, carried out at pH 7.5 (Figure 2), demonstrates a linear increase of signal area up to a vanadate/protein molar ratio of ca. 1.7/1, at which point a marked change in slope and the appearance of aqueous vanadate (-556 ppm) in the NMR spectrum indicates the completion of the titration. At ratios greater than 1.7 equiv of V(V) of Tf, the slope of signal area versus total V(V) (Figure 2a) is comparable to the slope of the signal area for an analogous "titration" in the absence of Tf (Figure 2b), although, not exactly equal to it. Furthermore, the signal area due to Tf-bound V(V) shows a slight decrease in this region. We attribute these effects to an equilibrium between bound and free V(V) in this concentration range (see below). That stoichiometric binding closer to a 2/1 ratio is not observed may also be affected by the coordination of adventitious metal ions (i.e., most likely Fe^{3+}) and the relatively small value of the V(V) binding constant estimated to be $\sim 10^{6.5}$ for each site.²

Figures 3 and 4 show the ^{51}V NMR spectra of aqueous vanadate, $\text{V}_1\text{-Tf}$ and $\text{V}_2\text{-Tf}$ at pH 9 and pH 5.8, respectively. The ^{51}V chemical shift of aqueous vanadate is strongly dependent on pH (Figures 1a, 3a, and 4a) reflecting the extent of protonation of orthovanadate, whereas the protein-bound resonances exhibit only very slight resonance shifts (1–2 ppm) (see Table I also). Furthermore, the line widths and chemical shifts of the protein-bound resonances are independent of protein concentration (10^{-4} – 10^{-3} M), nature of the buffer solution (Hepes, Bicine, Mes, unbuffered), and presence of excess free vanadate. The above experiments indicate unambiguously that the resonances at -529.5 and -531.5 ppm arise from protein-bound vanadium(V) which is in the limit of slow metal ion exchange on the NMR time scale (2.5×10^{-4} s).

Site Discrimination by NMR. The observation of two NMR signals with approximately equal signal intensity for V(V) bound to human transferrin indicates that ^{51}V NMR at 11.7 T can

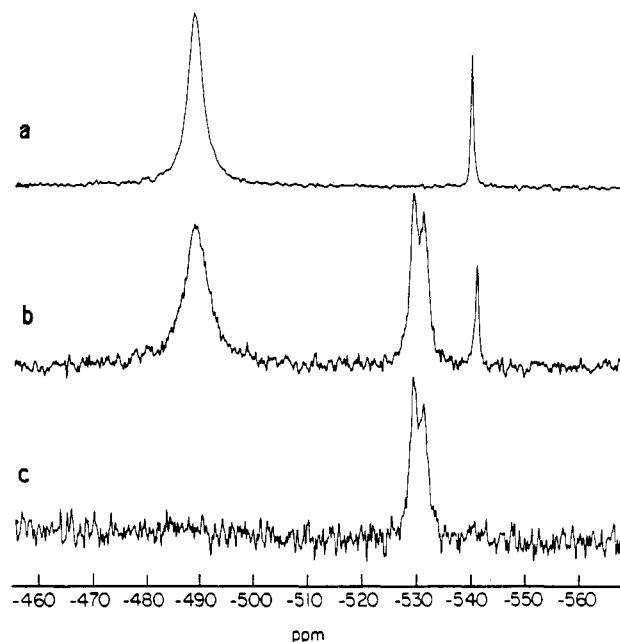


Figure 3. ^{51}V NMR spectra of V-Tf and vanadate at pH 9, 0.1 M Bicine buffer, 131.48 MHz: (a) 0.29 mM aqueous vanadate, 99 617 scans; (b) 2/1 V/apo-Tf at 0.29 mM apo-Tf, 145 958 scans; (c) equimolar mixture of vanadate and apo-Tf at 0.29 mM, 83 740 scans. The resonance at -490 ppm in (a) and (b) is due to a vanadium(V)-bicine complex, and the resonance at -542 ppm is HVO_4^{2-} .

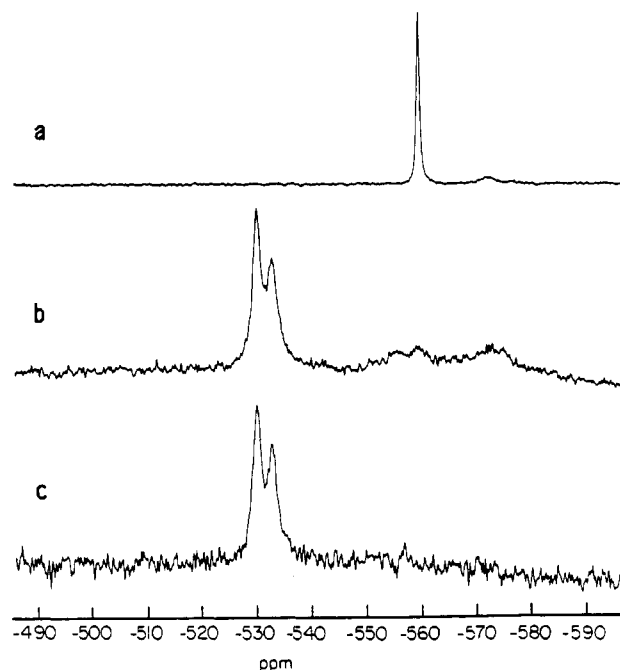


Figure 4. ^{51}V NMR spectra of V-Tf and vanadate at pH 5.3, 0.1 M Mes buffer, 131.48 MHz: (a) 0.29 mM aqueous vanadate, 26 386 scans; (b) 2/1 V/apo-Tf at 0.29 mM apo-Tf, 545 000 scans; (c) equimolar mixture of vanadate and apo-Tf at 0.29 mM, 208 659 scans. The broad resonances in the -570-ppm region of spectra a and b are due to exchanging oligovanadate species.

distinguish the C- and N-terminal binding sites by their distinct chemical shifts. A single resonance at -529.5 ppm is observed for V(V) addition to $\text{Fe}_\text{N}\text{-Tf}$ (pH 7.5, Hepes), suggesting that vanadium is bound to the C-terminal site, i.e., $\text{Fe}_\text{N}\text{V}_\text{C}\text{-Tf}$ (Figure 5). Similarly, a single protein-bound resonance at -533 ppm is produced when vanadate is added to $\text{Fe}_\text{C}\text{-Tf}$, indicating the formation of the $\text{V}_\text{N}\text{Fe}_\text{C}$ derivative (see Figure 2 of ref 4). The latter experiment was done at pH 5.8, since Fe(III) binds preferentially to the C-terminal site at this pH. The chemical shift

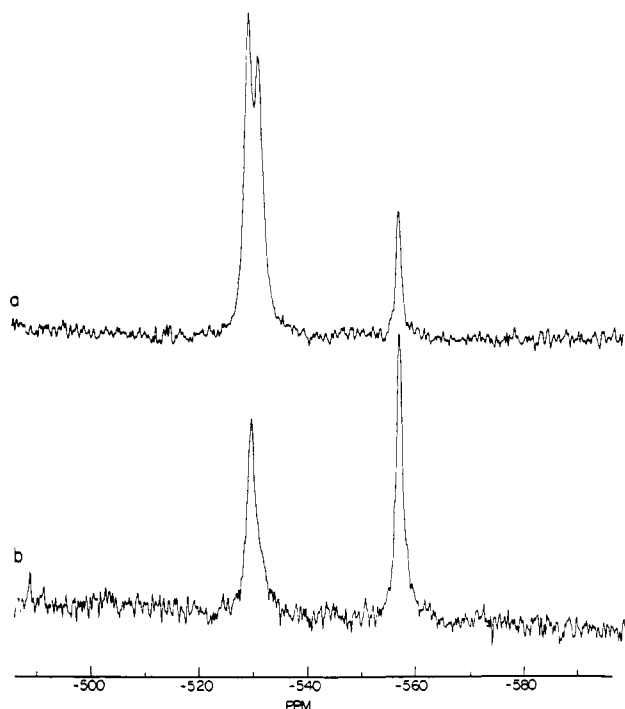


Figure 5. ^{51}V NMR evidence for identification of the V_C resonance, 131.48 MHz: (a) 0.78 mM $\text{V}_2\text{-Tf}$, pH 7.4, 0.1 M HEPES, 130080 scans; (b) equimolar mixture of vanadate and $\text{Fe}_\text{N}\text{-Tf}$ at 0.59 mM, pH 7.4, 0.1 M HEPES, 84008 scans.

of this sample is consistent with the position of the upfield protein resonance of $\text{V}_2\text{-Tf}$ at pH 5.8, also at -533 ppm (Figure 4b,c).

The two distinct resonances for vanadium(V) bound at the N- and C-terminal sites of human Tf indicate that the metal binding

Table I. NMR Parameters on the V(V)-Transferrin Complexes under Study at 131.5 MHz (11.7 T)^a

sample	concn (mM)	pH ± 0.1	δ_{iso} (ppm) ^b	$\Delta_{1/2}$ Hz ^c
$\text{V}_2\text{-transferrin}^d$	0.2-1.0	7.5	-529.5 -531.5 (-535 \pm 1.0) ^f	420 ^e (470 \pm 20) ^e
	0.29-0.69	9.0	-529.5 -531.4	400 ^e
	0.29	5.8	-529.8 -532.6	590 ^e
$\text{Fe}_\text{C}\text{V}_\text{N}\text{-transferrin}$	0.36-0.5	5.8	-532.0 (-536 \pm 1)	310 \pm 20 (500 \pm 20)
$\text{Fe}_\text{N}\text{V}_\text{C}\text{-transferrin}$	0.26-0.61	7.5	-529.6 (-535 \pm 1)	200 (470 \pm 20)

^aData obtained at 79.0 MHz (7.05 T) are given in parentheses. ^bResonance shift versus VOCl_3 ; ± 0.3 ppm unless specified. ^cFull width at half-height; ± 10 Hz unless specified. ^dNMR parameters of V(V)-Tf complexes were independent of the V/Tf ratio. ^eWidth of composite spectrum including both peaks. ^fChemical shift difference between V_C and V_N not resolvable at 7.05 T.

environments are similar but not identical. Vanadium bound at the N-terminal site is affected by temperature more than vanadium bound at the C-terminal site. The V_N resonance of $\text{V}_2\text{-Tf}$ and $\text{V}_\text{N}\text{Fe}_\text{C}\text{-Tf}$ shifts from -532.5 ppm at 275 K to -530.8 ppm at 310 K, whereas the V_C resonance shift of $\text{V}_2\text{-Tf}$ and $\text{V}_\text{C}\text{Fe}_\text{N}\text{-Tf}$ remains constant over this temperature range. This may indicate that the V_N coordination environment approaches that of the V_C site at higher temperatures. Further investigations of the nature of the temperature dependence of the V_N site are in progress.

Competitive Binding Studies. It has been shown previously by UV-vis spectroscopy that Fe(III) displaces V(V) from the binding sites of transferrin.² Figure 6 shows that ^{51}V NMR can also be used to monitor this reaction. Addition of iron(II) to an aerobic solution of $\text{V}_{1.8}\text{-Tf}$ (pH 7.5, 0.1 M HEPES, 0.01 M NaHCO_3) results in a decrease of the signal intensity due to Tf-bound V(V)

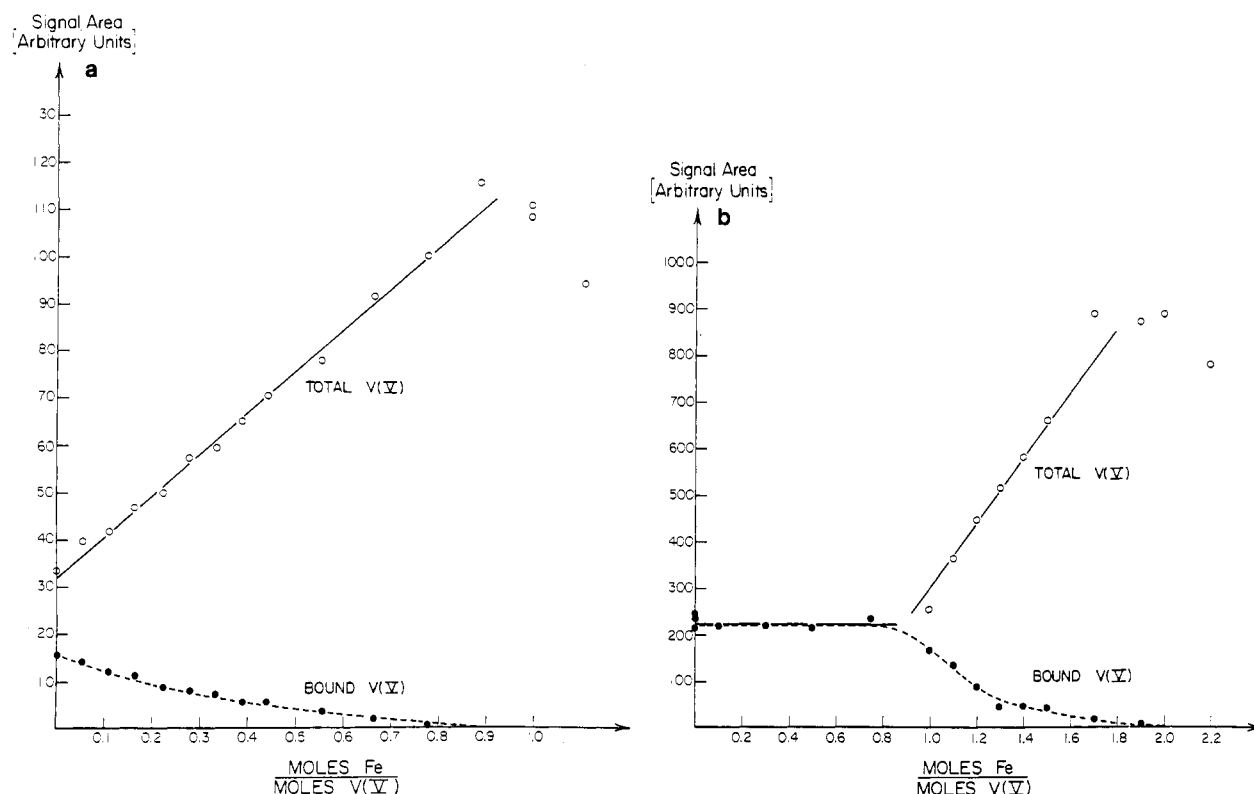


Figure 6. ^{51}V NMR evidence for the displacement of vanadium from $\text{V}_{1.8}\text{-Tf}$ by iron, 131.48 MHz: (a) titration of 0.71 mM $\text{V}_{1.8}\text{-Tf}$, (0.1 M HEPES, 0.01 M NaHCO_3 , pH 7.4) with an acidic solution of 0.0188 M $\text{Fe}^{\text{II}}(\text{NH}_4)_2(\text{SO}_4)_2$; (b) titration of 0.51 mM $\text{V}_1\text{-Tf}$ (0.1 M HEPES, 0.01 M NaHCO_3 , pH 7.4) with an acidic solution of 0.0188 M $\text{Fe}^{\text{II}}(\text{NH}_4)_2(\text{SO}_4)_2$. In part a, the total V(V) signal area is greater than the area due to bound V(V) before the addition of any iron because some aqueous vanadate is present in the $\text{V}_{1.8}\text{-Tf}$ spectrum. Part b shows that iron binds first to the vacant coordination positions before displacing bound V(V). Note that the total signal area due to V(V) increases during the titration reflecting the transition of bound V(V) (i.e., slow motion limit, reduced intensity) to free V(V) (i.e., extreme narrowing limit, full intensity).

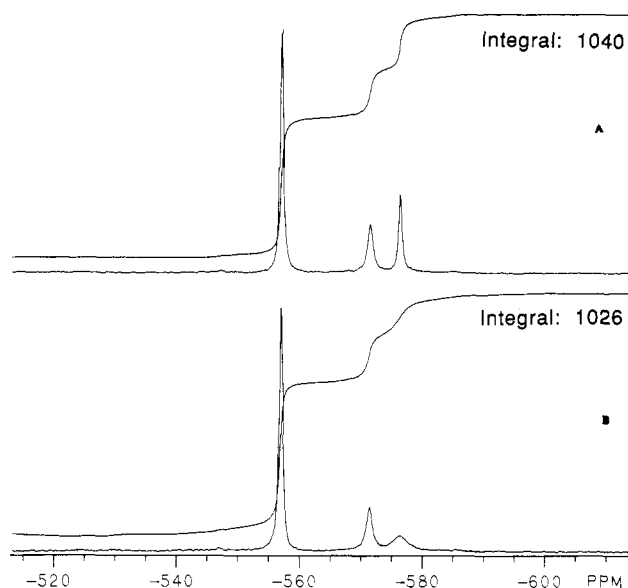


Figure 7. Effect of excess V(V) on the ^{51}V spectrum of $\text{V}_2\text{-Tf}$: (A) 1 mM solution of NH_4VO_3 (pH 7.5, 0.1 M Hepes), 10 000 scans; (B) 1 mM NH_4VO_3 (pH 7.5, 0.1 M Hepes), 0.05 mM Tf (V(V)/Tf = 20/1), 10 000 scans.

and the appearance of a new signal reflecting free vanadate species (Figure 6a). The same observation holds if iron is added to a solution of $\text{V}_1\text{-Tf}$, but only after the unoccupied sites first coordinate iron (Figure 6b). The protein-bound V(V) signal area decreases upon incremental addition of iron, with a concomitant increase in the aqueous vanadate resonance. The stoichiometric displacement of bound vanadium by iron is further evidence that V(V) is coordinated to Tf in the metal binding pocket.

Titration of $\text{V}_2\text{-Tf}$ with excess vanadate causes a progressive decrease in the Tf-bound vanadium signal. At ratios of about 20/1 V/Tf, very little protein-bound vanadium(V) is observed for 0.0125–0.38 mM Tf. Figure 7 shows that the integrated area of the ^{51}V spectrum of a 1 mM aqueous vanadate sample is identical with that of a solution of 1 mM vanadate with 0.05 mM apo-Tf (i.e., 20/1 V/Tf), within experimental error, demonstrating that all the V(V) is observed. A weak signal in the V–Tf region (–530 ppm) indicates some residual vanadium(V) coordination to Tf. The resonance of the tetravanadate species (–576 ppm) is broadened in all the transferrin-containing samples studied ([Tf] = 0.025–0.38 mM) with 20-fold excess vanadate, possibly owing to vanadium(V) exchange or nonspecific binding to transferrin under these conditions. Broadening of the –576-ppm resonance is more pronounced the higher the Tf and vanadate concentrations.

Removal of the polymeric vanadate species from the transferrin-containing solutions by extensive dialysis leads to quantitative recovery of the ^{51}V NMR signal due to protein-bound vanadate. This experiment confirms that the release of V(V) at high vanadate concentrations is not due to irreversible denaturation of the protein at high ionic strengths. The release may be due to either reversible conformational changes at the binding sites or due to increased rates of chemical exchange between bound and free vanadium as a result of the higher overall concentration of aqueous vanadate or as a result of nonspecific binding of tetrameric vanadate (Figure 7).

The UV–vis titration experiments of Harris and Carrano² and Chasteen³ do not indicate that bound vanadium is released upon addition of excess vanadate. However, their titrations did not exceed a 6-fold excess of vanadate and the Tf concentrations were significantly lower (0.01–0.028 mM Tf).^{2,3} At the resulting vanadium(V) concentrations, oligomerization does not occur.

The addition of anions (HCO_3^- , CO_3^{2-}), even in large excess, does not displace the bound V(V). These experiments eliminate the possibility that the observed ^{51}V NMR signals are due to V(V) bound to the anion binding sites and are consistent with Harris and Carrano's conclusion that vanadium is present as VO_2^{+2}

Addition of the anions H_2PO_4^- , SO_4^{2-} , and ClO_4^- also do not affect the transferrin-bound vanadium signal, although these anions cause substantial line broadening of the aqueous vanadate signal.

Quadrupolar Relaxation Characteristics. Previous solution-state ^{51}V NMR data have been analyzed and interpreted with the implicit assumption that the motional properties of the protein to which V(V) is bound place the metal ion into the extreme narrowing limit, i.e., $\omega_0\tau_c \ll 1$. Under such conditions, the spin–spin relaxation rate (which is proportional to the line width) is given by the expression

$$1/T_2 = (3/40)[(2I + 3)/\{I^2(2I - 1)\}]4\pi^2(e^2qQ/h)^2(1 + \eta^2/3)\tau_c \quad (1)$$

where e^2qQ/h is the nuclear electric quadrupolar coupling constant, η is the asymmetry parameter, and τ_c is the motional correlation time of the rotational diffusion. Assuming a spherical protein, König et al. estimated a correlation time, τ_c , of 2×10^{-7} s for transferrin²⁸ from the Stokes–Einstein equation. Uncritical application of eq 1, assuming a typical solid-state NMR value within the range of 0.5–5 MHz for the nuclear electric quadrupolar coupling constant, would predict a line width on the order of hundreds of kHz.⁴⁵ However, for our measurements on transferrin, eq 1 is irrelevant, since at our operating frequency of 131.48 MHz, $\omega_0\tau_c = 165$; i.e., the rotational diffusion is clearly outside the extreme narrowing.

It is well known that under such conditions the spin–spin relaxation of half-integer quadrupolar nuclei is multiexponential, giving rise to strong deviations from Lorentzian line shapes in the slow-motion regime.²⁹ For an $I = 7/2$ nucleus such as ^{51}V , the free-induction decay is a sum of four exponentials with individual relaxation times, provided that the motional narrowing condition ($\omega_{\text{int}}\tau_c \ll 1$) is still valid. Here ω_{int} refers to the strength of the anisotropic interactions governing the line shape in the rigid lattice limit. At high fields the latter is usually dominated by the chemical shift anisotropy, typical values of which range between 0 and 1500 ppm, depending on the symmetry of coordination.³⁰ Thus in our case $\omega_{\text{int}}\tau_c$ is on the order of 0.1 to 0.01 assuming König's value of τ_c . Therefore, in the absence of any local motion at the binding site, the protein-bound V(V) should lie well within the motional narrowing, while outside the extreme narrowing regime. This conclusion is confirmed by the sharpness of the ^{51}V NMR signal as well as the absence of other observable quadrupole transitions. Figure 8 depicts these individual spin–spin relaxation rates as a function of $\omega_0\tau_c$. In the limit of very long correlation times, the spin–spin relaxation rates of the components, II, III, and IV increase with increasing $\omega_0\tau_c$, leading to severe relaxation broadening.³¹ Note, however, the opposite behavior of component I whose spin–spin relaxation rate decreases over the same range resulting in a sharpening of this particular spectral component.

In addition, the theory describing quadrupolar relaxation outside of extreme narrowing conditions makes the following predictions.

(1) With increasing $\omega_0\tau_c$ the spin–spin relaxation rate of component I is expected to decrease, resulting in further sharpening until the motional narrowing condition is no longer fulfilled.

(2) The resonance position of component I should be affected by a second-order ("dynamic") frequency shift contribution.^{32,33} The magnitude of this contribution is inversely proportional to the external field strength³² and can thus be established by field-dependent shift measurements.

(3) If component I is the only observable spectral component, the absolute integrated intensity should amount to 19% of that of an equimolar vanadate solution.

(4) In the case of excessive broadening of the components II–IV, the effective precession frequency of the quadrupolar ^{51}V nuclei in the applied radio-frequency field might be affected.

(28) Koenig, S. H.; Schillinger, W. H. *J. Biol. Chem.* **1969**, *244*, 3283.

(29) Hubbard, P. S. *J. Chem. Phys.* **1970**, *53*, 985.

(30) Eckert, H.; Wachs, I. E. *Mater. Res. Soc. Symp. Proc.* **1988**, *111*, 459.

(31) Bull, T. E.; Forsen, S.; Turner, D. L. *J. Chem. Phys.* **1979**, *70*, 3106.

(32) Westlund, P. O.; Wennerstrom, H. *J. Magn. Reson.* **1982**, *50*, 451.

(33) Werbelow, L. G. *J. Chem. Phys.* **1979**, *70*, 5381.

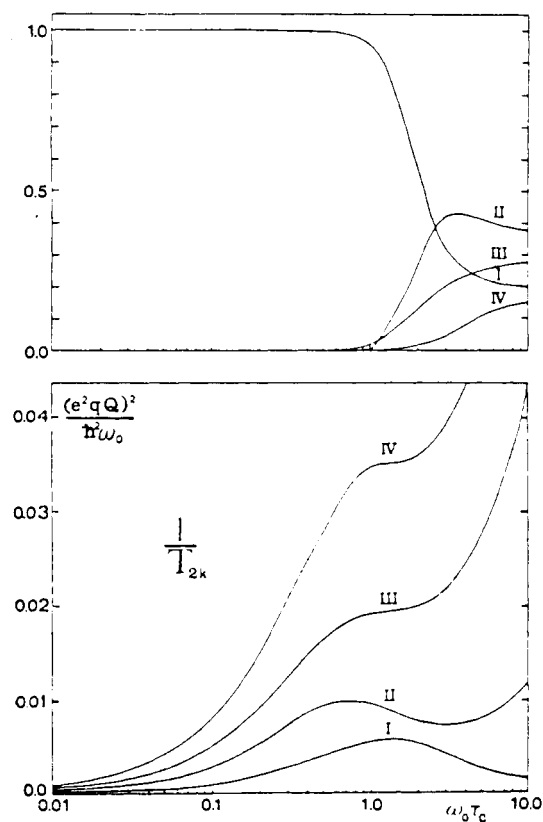


Figure 8. Transverse relaxation of spin $7/2$ nuclei in the absence of chemical exchange. The upper plot shows the amplitude of the four exponential components and the lower plot associated relaxation rates. Reproduced with permission from ref 31.

We have verified these predictions for V-Tf complexes with several V/Tf ratios, $\text{Fe}_N\text{V}_C\text{-Tf}$, and $\text{V}_N\text{Fe}_C\text{-Tf}$ by the following series of experiments described below.

Effect of Solvent Viscosity. Figure 9 shows the spectra of solutions of aqueous vanadate and $\text{V}_2\text{-Tf}$ titrated with glycerol. In concordance with eq 1, the resonances of the aqueous free vanadate species, which is in the extreme narrowing limit, broaden upon addition of glycerol reflecting the increase of τ_c with solvent viscosity. In addition, significant line shifts are observed which are due to complexation of V(V) by glycerol (i.e., -519 ppm), consistent with the observations of Tracey et al.¹⁴ In contrast, Figure 10 shows that, up to a certain limit, increasing the viscosity of the $\text{V}_2\text{-Tf}$ solution by addition of glycerol produces little change in width or position of the protein-bound ^{51}V signals. Our experiments on $\text{V}_2\text{-Tf}$, $\text{Fe}_N\text{V}_C\text{-Tf}$, and $\text{V}_N\text{Fe}_C\text{-Tf}$ indicate that this is true for both sites of the protein at 131.5 MHz and at room temperature. The slightly larger line width, 440 Hz, at the highest glycerol concentration studied (e.g., 50% v/v) may be due to residual anisotropic interactions that become noticeable as the assumption of the motional narrowing limit breaks down at extremely slow correlation times.

Effect of Magnetic Field Strength. As indicated in Table I, the line width measured at a lower magnetic field strength (7.05 T) is substantially larger than that measured at 11.7 T. Consistent with the prediction for the nonextreme narrowing case, this effect reflects the slower NMR time scale at the former field. The chemical shift difference between V_C and V_N sites is not resolved under these conditions. For both sites, the resonance position at 7.05 T is found about 5 ppm upfield of that measured at 11.7 T, independent of the V/Tf ratio and the presence of excess free vanadate. To our knowledge, this is the first clear-cut experimental observation of a second-order ("dynamic") frequency shift for a quadrupolar nucleus in an isotropic solution. [Marshall et al.³⁴

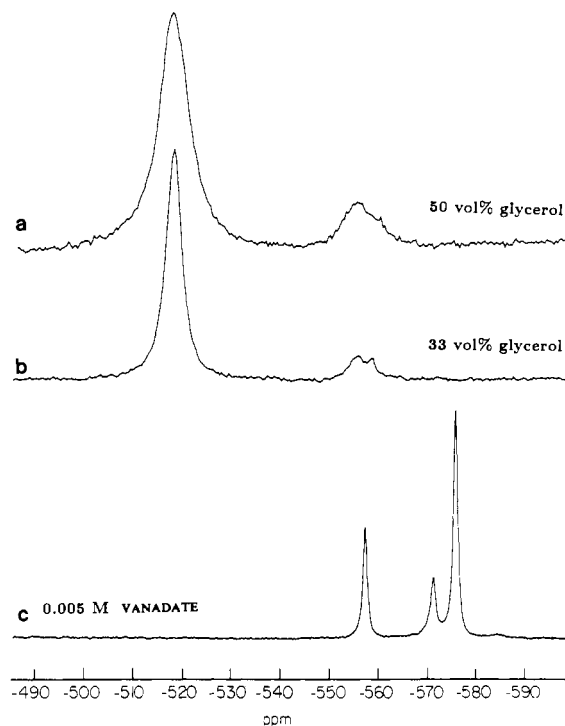


Figure 9. ^{51}V NMR spectra (131.48 MHz) of aqueous vanadate with and without glycerol, 0.1 M HEPES buffer, pH 7.4: (a) 2011 scans; (b) 3329 scans; (c) 18039 scans.

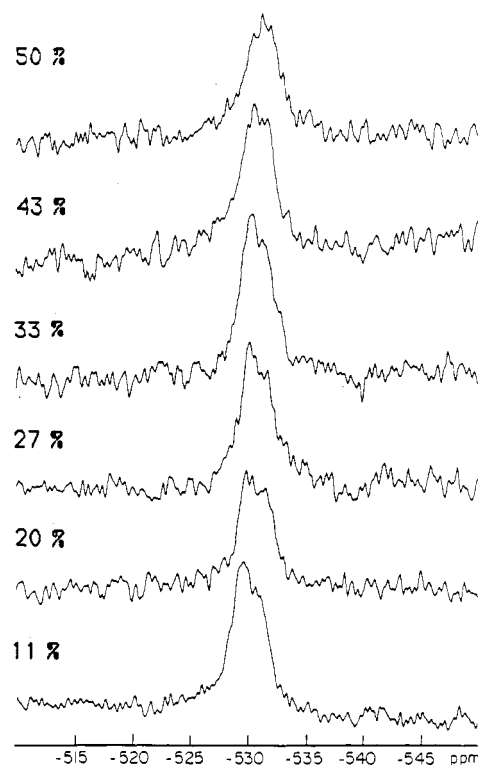


Figure 10. ^{51}V NMR spectra (131.48 MHz) of $\text{V}_{1.8}\text{-Tf}$ as a function of viscosity. Successive addition of glycerol to a 0.65 mM $\text{V}_{1.8}\text{-Tf}$, 0.1 M HEPES, pH 7.4 at 11% (50 000 scans), 20% (100 000 scans), 27% (100 000 scans), 33% (200 000 scans), 43% (200 000 scans), and 50% (215 187 scans) glycerol (v/v). Spectra are scaled to equal heights.

have used DISPA plots to identify NMR dynamic frequency shifts in a suspension of NaCl in sodium/lauric acid micelles. This interpretation has been disputed in later work.³⁵

Signal Quantitation and Pulse Angle Dependence. In our previous communication we had noted that the integrated signal

(34) Marshall, A. G.; Wang, T. C. L.; Cottrell, C. E.; Werbelow, L. G. *J. Am. Chem. Soc.* **1982**, *104*, 7665.

(35) Lerner, L.; Torchia, D. A. *J. Am. Chem. Soc.* **1986**, *108*, 4264.

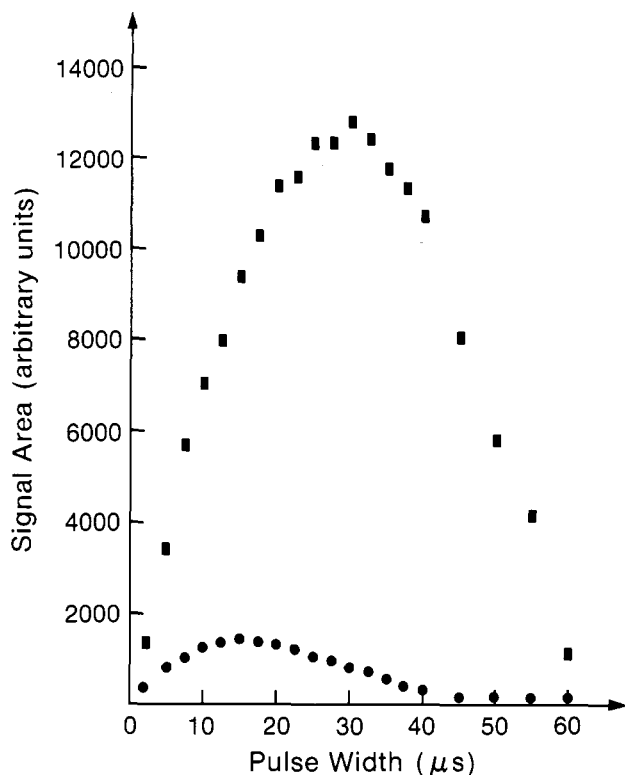


Figure 11. Integrated ^{51}V NMR signal area (131.48 MHz) as a function of pulse width: 0.51 mM $\text{V}_1\text{-Tf}$ (circles) and an equimolar solution of aqueous vanadate (squares). The frequency carrier was placed exactly on resonance in each experiment. Note that the signal area of Tf-bound vanadate is maximized at a shorter pulse length than the signal of aqueous vanadate.

intensity of Tf-bound $\text{V}(\text{V})$, carried out at a pulse length that maximized the free induction decay intensity of the bound species, was ca. 15% of that of an equimolar solution of aqueous vanadate. Upon reinvestigation we confirmed this result but discovered that the effective precession frequencies in the rotating frame for the bound and free vanadate are different. Figure 11 illustrates the dependence of integrated signal area as a function of pulse length at a radio-frequency field strength, ω_1 , of 8.3 kHz. Thus the pulse length that maximizes free induction decay intensity for the bound $\text{V}(\text{V})$ is found at approximately one-half of the 90° pulse length measured for an aqueous vanadate solution. The origin of this effect lies in a selective excitation phenomenon. Using a fictitious spin $1/2$ formalism,³⁶ it has been shown that in the weak irradiation case, $\omega_1 \ll \omega_Q$, the length of a 90° pulse, t_p , applied selectively to the central transition of half-integer quadrupolar nuclei is given by

$$\Pi/2 = (I + 1/2)\omega_1 t_p \quad (2)$$

Here, ω_1 is the radio-frequency field strength and ω_Q is proportional to the nuclear electric quadrupolar constant.³⁶ This "flip-angle" effect has been frequently observed in solid-state NMR studies of quadrupolar nuclei^{37,38} and was, more recently, used to prove the presence of residual quadrupole splittings in liquid crystalline systems.³⁹ We attribute this effect to incomplete spectral excitation of the quadrupolar relaxation components II, III, and IV (see Figure 8), which are broadened excessively due to relaxation. We believe that this is the first experimental observation of such an effect in an isotropic solution. Equation 2 predicts that the 90° pulse length, t_p , for a nucleus with spin $7/2$ where all of the allowed transitions are excited, should be shortened

(36) Vega, S. *J. Chem. Phys.* **1978**, *68*, 5518. Wokaun, A.; Ernst, R. R. *J. Chem. Phys.* **1977**, *67*, 1752.

(37) Kentgens, A. P. M.; Lemmens, J. J. M.; Geurts, F. M. M.; Veeman, W. S. *J. Magn. Reson.* **1987**, *71*, 62.

(38) Man, P. P.; Theveneau, H.; Papon, P. *J. Magn. Reson.* **1985**, *64*, 271.

(39) Joseph, P. M.; Summers, R. M. *Magn. Res. Med.* **1987**, *4*, 67.

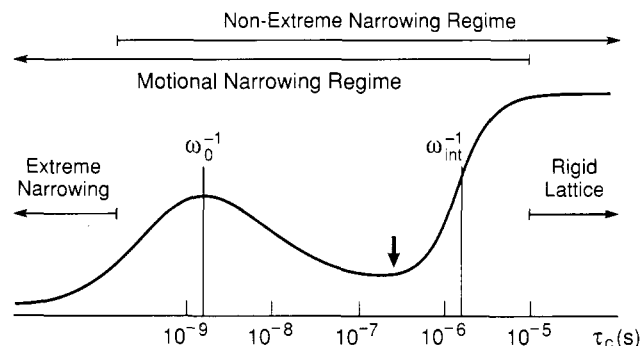


Figure 12. Schematic illustration of the qualitative dependence of the central $1/2 \rightarrow -1/2$ transition line width on the correlation time τ_c . The estimated correlation time for transferrin is indicated by an arrow.

to $t_p/4$ if only the central transition is excited. From the smaller reduction in 90° pulse length actually observed, we conclude that this extreme situation does not occur and that components II, III, and IV may be excited to some degree. Indeed, the reduction of the effective pulse length for the Tf-bound species is less pronounced, although still present when ω_1 is increased to 27.8 kHz.⁴⁰ Figure 11 illustrates that, as a consequence, the fraction of observable signal due to bound $\text{V}(\text{V})$ compared to that of an equimolar solution of aqueous vanadate, now depends on the applied pulse length, but remains approximately constant in the limit of very short flip angles, where it approaches the theoretical limit of 19%. This behavior conforms with theoretical calculations carried out by Lippmaa and co-workers for the analogous case in solid-state NMR.⁴¹ Furthermore, our studies indicate that the excitation spectra for the V_N and the V_C sites are identical at room temperature and independent of the V/Tf ratio.

Discussion and Conclusions

The Vanadium Coordination Site. While the value of the ^{51}V NMR chemical shift of $\text{V}_2\text{-Tf}$ cannot be used to identify the nature of all the metal-binding ligands, the ^{51}V chemical shift in the -530 -ppm region falls within the range of several $\text{V}(\text{V})$ phenolate-containing molecules, indicating that tyrosine coordination in $\text{V}_2\text{-Tf}$ is likely. The ^{51}V NMR chemical shift of $\text{V}(\text{V})(\text{O})(\text{ethylenebis}(\text{salicylidenediamine}))$ (VOSalen) occurs at -471 ppm in Me_2SO ,⁴³ $\text{V}(\text{V})(\text{O})_2\text{ethylenebis}(o\text{-hydroxyphenyl})\text{glycine}$ (VO_2EHPG) occurs at -540 ppm in Me_2SO ,^{42,43} $\text{V}(\text{V})\text{O}_2\text{-salicylidenediaminato-}N^2(2\text{-hydroxyethyl})\text{ethylenediamine}$ occurs at -528 ppm in Me_2SO ,^{42,44} and $\text{V}(\text{V})\text{O}_2\text{-salicylaldehyde-L-aspartate}$ occurs at -496 ppm in 80/20 ethanol/water.⁴² Tyrosinate coordination is also supported by Harris and Carrano's analysis of the magnitude of the extinction coefficient changes at 260 nm upon $\text{V}(\text{V})$ addition to apo-Tf.² They predicted coordination of two tyrosine residues which is consistent with the recent crystal structure of $\text{Fe}_2\text{-lactoferrin}$ showing that only two of the three conserved tyrosine residues in the metal binding region are coordinated to $\text{Fe}(\text{III})$.⁵ Harris and Carrano conclude further that vanadium is present as VO_2^+ by comparison of the lack of an absorption maximum in the visible region with the electronic spectra of other vanadium(V) compounds.² The stoichiometric displacement of $\text{V}(\text{V})$ by iron in the presence of bicarbonate is further evidence that $\text{V}(\text{V})$ is coordinated at the metal binding site and not bound at the carbohydrate moieties. As we noted above, anions (e.g., carbonate, phosphate, sulfate, perchlorate)

(40) It should be possible to characterize the excitation spectrum of the bound vanadate by using the new method of 2-D nutation spectroscopy recently introduced by Kentgens et al.³⁷

(41) Samoson, A.; Lippmaa, E. *Phys. Rev. B.* **1983**, *28*, 6567.

(42) de La Rosa, R. I.; Butler, A., work in progress.

(43) Bonadies, J. A. Ph.D. Dissertation, University of Vermont, 1988. We thank J. A. Bonadies and C. J. Carrano for providing the sample of $\text{V}(\text{V})(\text{O})_2\text{ethylenebis}(o\text{-hydroxyphenyl})\text{glycine}$ (VO_2EHPG).

(44) We thank V. L. Pecoraro for providing the sample of $\text{V}(\text{V})\text{O}_2\text{-salicylidenediaminato-}N^2(2\text{-hydroxyethyl})\text{ethylenediamine}$ ($\text{V}(\text{V})\text{-O}_2\text{SHED}$). Li, X.; Lah, M.S.; Pecoraro, V. L. *Inorg. Chem.* **1988**, *27*, 4657.

do not displace coordinated vanadium(V), indicating that V(V) is not bound at the anion binding sites.

Criteria for Observable Sharp ^{51}V NMR Lines in Tightly Bound Systems. The observation of sharp ^{51}V NMR signals in the present study contrasts with earlier work in which the signals of protein-bound vanadate were found to be very broad or even unobservable.^{13,22–25} While at the present time our studies do not enable us to predict ^{51}V NMR line widths quantitatively, the following qualitative discussion, in conjunction with the scheme of Figure 12 might serve as a useful guide in the search for other suitable metal–protein systems. In general, the feasibility of ^{51}V NMR in such systems will depend on the location of τ_c with respect to the window of motional correlation times between ω_0^{-1} and ω_{int}^{-1} . This is, to some extent, under the control of the experimenter. Clearly, Figure 8 suggests the use of the highest possible magnetic field strength. On the other hand, the same effect can, in principle, be obtained by increasing τ_c by lowering the temperature, increasing solvent viscosity, or attaching the atom or molecule under study to a large macromolecule. This strategy of deliberately slowing down the reorientational motion in a liquid contrasts sharply with the opposite approach frequently taken in the extreme narrowing limit, where efforts are aimed at decreasing correlation times by either raising the temperature or using low viscosity solvents.

In addition, the feasibility of ^{51}V NMR will depend on the minimum achievable line width within this window, which is essentially a function of the electric gradient tensor at the site of the ^{51}V nucleus and the ^{51}V NMR line width outside of the motional narrowing limit. The latter is usually governed by either the ^{51}V chemical shift anisotropy or (at low fields) second-order quadrupolar perturbations, and thus depends also on the external field strength used. In general, sharp lines are expected for symmetric environments with small quadrupolar coupling constants and chemical shift anisotropies. However, it is clear from the above discussion, that under nonextreme narrowing conditions the

external magnetic field strength plays a much more crucial role in balancing the effects of relaxation broadening and static broadening, and thus ^{51}V NMR signals observable at 11.7 T might in certain cases be broadened beyond detectability at a field strength of 1.4 T or vice versa.

Implications of the Nonextreme Narrowing Condition for Quantitative Spectroscopic Applications. In the present study, the nonextreme narrowing condition results in the benefit of excellent spectroscopic resolution which for most ^{51}V NMR applications is usually not achievable in the extreme narrowing limit. On the other hand, this motional regime impacts certain quantitative spectroscopic aspects of quadrupolar solution-state NMR, which have to be borne in mind in future applications. First, the detection sensitivity is decreased by a factor of 5 (for $I = 7/2$), hence requiring the use of more concentrated solutions. In the case of ^{51}V NMR of proteins we estimate a lower detection limit of 0.05 mM in 10-mm NMR tubes on 11.7-T magnets. Additional complications arise from the flip-angle effect. Future chemical applications will require systematic monitoring of the pulse angle dependence over the entire chemical process to be studied and quantitative accounting for any changes observed in the excitation spectrum. Finally, chemical shifts will have to be viewed with some caution, since dynamic frequency shifts will contribute to the resonance positions measured. The latter can be evaluated by field-dependent measurements and at the maximum available field strength. Notwithstanding these methodological constraints, quadrupolar central transition NMR in the nonextreme narrowing limit is expected to offer many interesting new possibilities in future studies of metal protein interactions.

Acknowledgments. A.B. acknowledges grants from the National Institutes of Health (GM-38130) and the Petroleum Research Fund of the American Chemical Society. A.B. acknowledges helpful discussions with N. D. Chasteen. We also acknowledge helpful discussions with J. P. Yesinowski. Some of the NMR studies were carried out at the Southern California Regional NMR Facility, funded by NSF Grant No. CHE 84-40137.

(45) Rehder, D. *Inorg. Chem.* 1988, 27, 4312. See ref 10 herein.

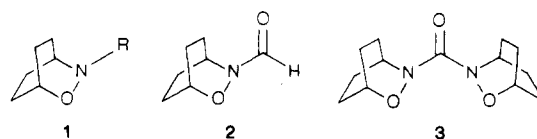
ESR and Optical Study of Electron Transfer between the NO Units of an N,N' -Dialkoxyurea Cation Radical

Stephen F. Nelsen,^{*,†} James A. Thompson-Colon,[†] and Menahem Kafkory[‡]

Contribution from the S. M. McElvain Laboratories of Organic Chemistry, Department of Chemistry, University of Wisconsin, Madison, Wisconsin 53706, and Department of Chemistry, Technion—Israel Institute of Technology, Haifa 32000, Israel. Received June 16, 1988

Abstract: Carbonylbis[3-(2-oxa-3-azabicyclo[2.2.2]octane)] (**3**) has a ν_{IP} of 8.20 eV and E° of 1.17 V vs saturated calomel electrode (0.1 M $n\text{-Bu}_4\text{NClO}_4/\text{CH}_3\text{CN}$). The X-ray structure of crystalline **3**, which exists in a conformation with one NO group *Z* and the other *E* to the carbonyl group, is reported. **3** gives a cation radical having its "hole" instantaneously localized on one NO unit. Analysis of the low-temperature ESR spectra of $3^{+\cdot}$ in CH_2Cl_2 for electron transfer between two equivalent sites gave ΔG_{th}^* near 3.5 kcal/mol between -84 and -30 °C. $3^{+\cdot}$ exhibits a near-IR charge-transfer band which varies between 1320 nm in CHCl_3 and 1260 nm in CH_3CN , and the band energy versus Marcus γ value plot for five solvents is linear, as expected for instantaneous hole localization. Extrapolation of this plot to $\gamma = 0$ gives a value of λ_{i} of 20.5 kcal/mol, producing a λ_0 value of 2.1 kcal/mol in acetonitrile using Hush theory.

The 2-oxa-3-azabicyclo[2.2.2]octyl ring system **1-R** has proven useful for study of electron loss equilibria as the R group is changed. The bicyclic ring system Bredt's rule kinetically protects hydrogen loss α to both heteroatoms of the alkoxyamine unit, and long cation-radical lifetimes are observed even when R is a pow-



erfully electron-withdrawing carbonyl group and electron loss is thermodynamically difficult.¹ A principal conclusion from a study

[†]University of Wisconsin.

[‡]Technion—Israel Institute of Technology.